ELSEVIER

Polymer 42 (2001) 1083–1094

polymer

www.elsevier.nl/locate/polymer

Nylon 6 nanocomposites by melt compounding

J.W. Cho, D.R. Paul*

Department of Chemical Engineering and Texas Material Institute, University of Texas at Austin, Austin, TX 78712, USA

Received 24 February 2000; received in revised form 10 May 2000; accepted 10 May 2000

Abstract

Nylon 6–organoclay nanocomposites were prepared via direct melt compounding using a conventional twin screw extruder. The mechanical properties and morphology of these nanocomposites were determined and compared to similar materials made by an in situ polymerization process. The organoclay was well exfoliated into the nylon 6 matrix when compounded with the twin screw extruder but use of a single screw extruder was far less effective. The mechanical properties of the organoclay nanocomposites were significantly increased with marginal decrease of ductility and showed much greater values than glass fiber composites.

Keywords: Nylon 6/clay nanocomposite; Montmorillonite; Quaternary ammonium cation

1. Introduction

A variety of inorganic materials, such as glass fibers, talc, calcium carbonate, and clay minerals, have been successfully used as additives or reinforcement to improve the stiffness and strength of polymers. The extent of property enhancement depends on many factors including the aspect ratio of the filler, its degree of dispersion and orientation in the matrix, and the adhesion at the filler–matrix interface. Generally, inorganic materials neither have good interaction with organic polymers to achieve good dispersion nor adequate adhesion, and, as a result, surface treatments are common. Mica-type silicates like montmorillonite, hectorite, and saponite have received a great deal of attention recently [1–3] as reinforcing materials for polymers owing to their potentially high aspect ratio and unique intercalation/exfoliation characteristics. Such clay minerals have a layer structure (typically ~1 nm in thickness) which if properly exfoliated can lead to platelets (approaching 1 μm in lateral dimensions) with very high stiffness and strength dispersed in the polymer matrix. To achieve a better interaction with organic polymers, the cations (typically sodium) present on the surface of montmorillonite to balance the net negative charge of the aluminum/magnesium silicate layer are exchanged with organic molecules with a cation group, e.g. alkyl ammonium ions to produce an organoclay.

The incorporation of organoclays into polymer matrices has been known for 50 years. In 1950, Carter et al. [4] developed organoclays with several organic onium bases to reinforce latex-based elastomers. In 1963, the incorporation of organoclay into a thermoplastic polyolefin matrix was disclosed by Nahin and Backlund of Union Oil Co. [5]. They obtained organoclay composites with strong solvent resistance and high tensile strength by irradiation induced crosslinking. However, they did not focus on the intercalation characteristics of the organoclay or the potential properties of the composites. In 1976, Fujiwara and Sakomoto [6] of the Unichika Co. described the first organoclay hybrid polyamide nanocomposite. One decade later, a research team from Toyota disclosed improved methods for producing nylon 6–clay nanocomposites using in situ polymerization similar to the Unichika process [7–10]. They also reported on various other types of polymer–clay hybrid nanocomposites based on epoxy resin, polystyrene, acrylic polymer, rubber, and polyimides formed using a similar approach [11–15]. They reported that these polymer–clay nanocomposites exhibit superior strength, modulus, heat distortion temperature, water and gas barrier properties, and with comparable impact strength as neat nylon 6 [13,15–19]. Numerous research groups have also described clay nanocomposites based on a variety of polymers including polystyrene [20–22], epoxy resin [23–25], poly(methyl methacrylate) [26], polycaprolactone [27,28], polyolefins [29–32], polyurethanes [33], polyimides [34], among others.

According to Vaia et al. [20,21,35,36], nanocomposites can be obtained by direct polymer melt intercalation where polymer chains diffuse into the space between the clay

* Corresponding author. Tel.: +1-512-471-5392; fax: +1-512-471-0542.
E-mail address: drp@che.utexas.edu (D.R. Paul).

0032-3861/01/$ - see front matter
PII: S0032-3861(00)00380-3

Table 1
Material used in this study

Material	Commercial name	Description	Supplier
Nylon 6	B135WP	$\bar{M}_n = 29,300$[a]	AlliedSignal
Montmorillonite (MMT)	Cloisite Na(+)	Cation exchange capacity = 95 mequiv./100 g	Southern Clay Products
Organoclay (OCL)	SCPX 2004	Treated with a quaternary ammonium cation	Southern Clay Products
Nylon 6/glass fiber	Durethan BKV 30	30 wt.% glass fiber	Bayer

[a] From intrinsic viscosity measurement using $[\eta] = 5.26 \times 10^{-4} \overline{M}_w^{-0.745}$ assuming $\overline{M}_n = 1/2\overline{M}_w$.

layers or galleries. They suggest that this approach can be combined with conventional polymer processing techniques such as extrusion to decrease the time to form these hybrids by breaking up clay particles and increasing sample uniformity.

The incorporation of organoclays into thermoplastic matrices by conventional polymer melt compounding processes is a promising new approach for forming nanocomposites that would greatly expand the commercial opportunities for this technology. If technically possible, melt compounding would be significantly more economical and simple than in situ polymerization processes. This approach would allow nanocomposites to be formulated directly using ordinary compounding devices such as extruders or other mixers according to need without the necessary involvement of resin producers. However, there are very few studies on formation of nanocomposites by direct melt compounding [37–40]; and, therefore, the corresponding knowledge about this process and what can and cannot be accomplished is still very incomplete. In this process, the rheological and thermodynamic character of the materials can be important parameters that affect the degree of exfoliation and properties of the final composites. The dispersion of filler agglomerates can be achieved when the cohesive forces of the agglomerates are exceeded by the hydrodynamic separating forces applied by the matrix fluid [41]. In the case of the intercalated organoclay, the amount of exfoliation appears to be strongly affected by the conditions of mixing. Generally, the degree of dispersion is governed by the matrix viscosity, average shear rate, and the mean residence time in the mixing process.

In a recent study, we describe the preparation of nylon 6 nanocomposites by melt compounding and investigate their degree of exfoliation and mechanical properties in terms of the type of organoclay, extruder and screw configuration [42]. We have found that the mechanical properties of nylon 6 nanocomposites are affected by the degree of exfoliation, which is dependent on both processing conditions and the clay chemical treatment.

In this paper, we explore nylon 6 nanocomposites formed by melt compounding and compare their properties with other nancomposites and glass fiber reinforced composites. We also investigate optimization of processing parameters such as processing temperature, residence time, and amount of shear.

2. Experimental

The nylon 6 used in this study is a commercially available material from AlliedSignal with $\overline{M}_n = 29,300$. The clay minerals were supplied by Southern Clay Products. Sodium montmorillonite (MMT) was received as a fine powder with an average particle size of 7 μm with a cation exchange capacity (CEC) of 95 mequiv./100 g. The organoclay (OCL) was formed by ion exchange of sodium montmorillonite with bis(hydroxyethyl) (methyl) rapeseed alkyl ammonium chloride. It contains 63 wt% of clay mineral. This experimental product was recommended by Southern Clay Products for initial studies. Further work will follow on other organoclays. A glass fiber reinforced material with a comparable amount of filler was prepared from a commercial nylon 6/glass fiber 70/30 composite. More details about the materials used are given in Table 1. Prior to each processing step, all polyamide containing materials were dried in a vacuum oven for at least 16 h at 80°C to avoid moisture induced degradation reactions.

Composites were prepared by melt compounding using two different extruders. The majority of the nanocomposites were prepared using a Haake intermeshing co-rotating twin screw extruder with a 30 mm diameter screw having a centerline spacing of 26 mm and a 305 mm screw length. The screw configuration contains two kneading disc blocks located at 35 and 147 mm, respectively, from the hopper. Both kneading disc blocks consist of one right-handed medium-pitched ($L/D = 1.0$), one left-handed medium-pitched ($L/D = 1.0$) kneading disc elements and one mixing ring. Most of the compounding was carried out using a barrel temperature of 240°C, screw speed of 180 rpm, and a feed rate of 920 g/h. The mean value of the residence time for neat nylon 6 at this condition is 5.3 min.

For comparative purposes, a Killion single screw extruder was used. This machine has a 25.4 mm diameter screw with two intensive mixing heads ($L/D = 1$) and a 762 mm screw length. Compounding was carried out at 240°C using a screw speed of 40 rpm. The mean value of the residence time in this extruder for neat nylon 6 at this condition is

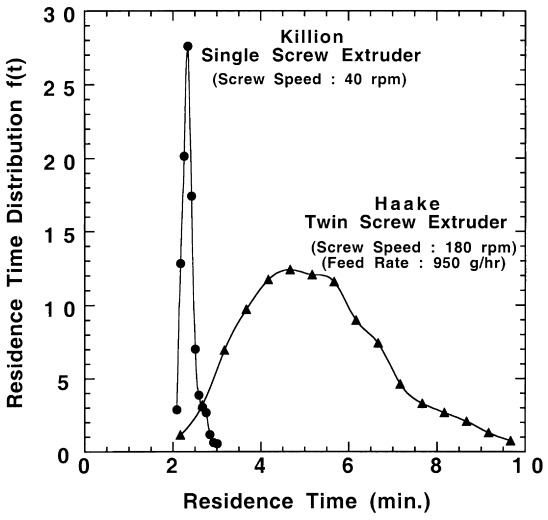

Fig. 1. Residence time distribution curves at the die exit for the single screw extruder at 40 rpm and for the modular intermeshing co-rotating twin screw extruder at 180 rpm.

2.35 min. The residence time distribution of the two extruders is shown in Fig. 1.

The extruded pellets were injection molded into standard 0.318 cm thick Izod (ASTM D256) and tensile (ASTM D638 type I) bars using an Arberg Allrounder injection molding machine. The barrel temperature was set at 260°C and the mold temperature at 80°C. An injection pressure of 70 bar and a holding pressure of 35 bar were used. Detailed processing conditions are described in Table 2.

The shear viscosity of the individual composites was determined at 240°C with an Instron Capillary Rheometer. Thermal properties were studied by DSC and TGA using a Perkin–Elmer DSC 7 equipped with a thermal analysis data station, operating at a heating rate of 20°C/min in a nitrogen atmosphere. The sample was first heated at 240°C and held for 5 min to remove previous history. The sample was then cooled to −50°C at a rate of 20°C/min. The T_g was determined as the inflection point of the glass transition region on the DSC thermogram.

Table 2
Processing conditions used in this study

Equipment type	Processing conditions	Manufacturer
Single screw extruder	Screw speed: 40 rpm Barrel temp.: 240°C Feed rate: fully fed	Killion
Modular intermeshing co-rotating twin screw extruder	Screw speed: 180 rpm Barrel temp.: 240°C Feed rate: 920 g/h	Haake
Injection molding	Screw speed: 150 rpm Barrel temp.: 260°C Injection pressure: 70 bar Holding pressure: 35 bar Molding temperature: 80°C	Arburg Allrounder

X-ray diffraction (XRD) measurements were made directly from montmorillonite and organoclay powders. In the case of the nanocomposites, measurements were carried out on films. All these experiments were performed using a Sintag XDS 2000 diffractometer.

The morphology of nylon 6 nanocomposites was imaged using a Phillips/EM 301 transmission electron microscope (TEM). Ultra-thin sections (5 nm) were cut from Izod bars perpendicular to the flow direction under cryogenic conditions using a Reichert-Jung Ultracut E microtome.

All specimens were kept in a sealed desiccator under vacuum for 24 h before mechanical property measurements were performed. The values reported reflect an average from five measurements. Tensile testing was done using an Instron at a crosshead speed of 0.508 cm/min for modulus and yield strength measurements and 5.08 cm/min for elongation at break measurements. Notched Izod impact strength was determined using a TMI pendulum-type impact tester equipped with an insulated chamber for heating and cooling the specimens.

3. Melt exfoliation

Fig. 2 shows X-ray powder diffraction patterns for the organoclay powder and composites with nylon 6 formed in the single and twin screw extruders. Fig. 3 shows an SEM photomicrograph of organoclay particles (part a) and TEM photomicrographs of nanocomposites prepared in two different extruders (parts b–e). The particle shape of the organoclay powder (Fig. 3a) indicates a plate-like structure with an average particle diameter of about 6 μm. As indicated in Fig. 2, the interlayer platelet spacing of this organoclay (d_{001} diffraction peak) is about 18 Å.

For the composite prepared by single screw extrusion, full exfoliation is not achieved most likely because the amount of shear is insufficient and the residence time is too short. As seen in Fig. 3b, there are undispersed particles of organoclay remaining and many silicate layers in an ordered tactoid structure are observed in the vicinity of clay particles. However, some portions of the organoclay are locally well exfoliated (see high magnification in Fig. 3c). Consequently, the final product is a mixture of exfoliated and conventional clay composites. The XRD pattern of this composite, Fig. 2, curve b, exhibits two broad diffraction peaks. One is characteristic of the original organoclay with basal spacing of 18 Å and the other is a broad new peak corresponding to the layer separation of organoclay in the matrix; both peaks are rather low in intensity compared to the neat organoclay.

Fig. 3d and e shows TEM images of a nylon 6/clay nanocomposite prepared in the twin screw extruder. The low magnification view in Fig. 3d reveals that the organoclay is uniformly dispersed into nylon 6. Fig. 3e shows a higher magnification picture that reveals that the organoclay is well exfoliated in the nylon 6 matrix and the individual layers are

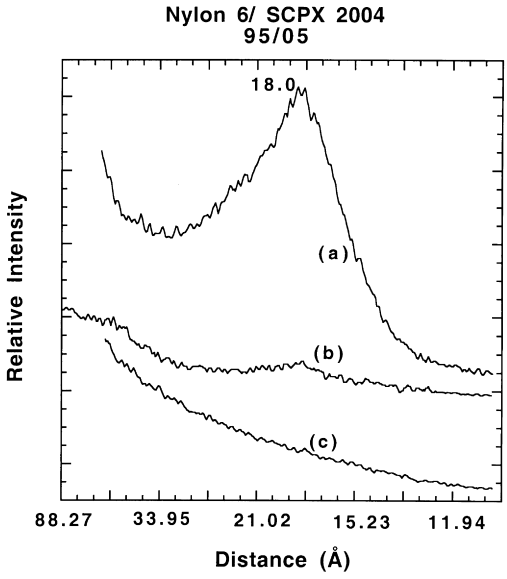

Fig. 2. X-ray diffraction scans for (a) organoclay powder and nylon 6/ organoclay 95/05 nanocomposites prepared by melt compounding in (b) the single screw extruder and (c) the twin screw extruder.

aligned along the flow axis. The absence of the characteristic clay d_{001} diffraction peak in Fig. 2 is also strong evidence for the formation of an exfoliated nanocomposite. The dark lines in Fig. 3e are the crosssections of single or possibly multiple silicate platelets. The platelets are flexible and, thus, show some curvature. The average thickness of the clay platelets appears to be approximately 3 nm while the average length is about 120 nm. The thickness deduced from these photomicrographs is somewhat higher than that of a single clay layer, which should be about 1 nm. There are several possible reasons for this discrepancy. One possibility is the clay platelets are not fully exfoliated. Another possibility is that the platelets appear in the image to be larger than they actually are due to inaccurate focusing in the TEM. A third possibility is that the microtoming direction is not perfectly perpendicular to the surface of the platelets so the image is of a tilted platelet that appears to be thicker than it actually is. Future work will attempt to address these possibilities.

4. Rheology

For polymer composite systems, the size, shape and concentration of the filler can have a significant effect on the rheological properties in the melt state. Generally, the viscosity of molten reinforced composites exhibit shear thinning behavior at high shear rates; however, at low shear rates the viscosity usually increases with filler concentration and may even show an yield value. However, there have been relatively few detailed studies of the rheological properties of nanocomposites formed from organoclays [43–46]. Fig. 4 shows the shear viscosity behavior of neat nylon 6 and the various composites at high shear rates measured by capillary rheometry. The nanocomposite formed from the organoclay exhibits similar shear thinning behavior as neat nylon 6 and the composites with the same amount of glass fiber or unmodified montmorillonite. It is of great interest to note that the absolute value of the melt viscosity of the organoclay nanocomposite is significantly lower than that of neat nylon 6 or the other composites shown. The low viscosity of the nanocomposite implies good melt processability over a wide range of practical processing conditions such as extrusion and injection molding. However, it is not clear what mechanism causes the reduction of melt viscosity in the nanocomposite. One possibility is slip between the nylon 6 matrix and the exfoliated organoclay platelets during high shear flow. Another possibility is a reduced molecular weight of the nylon 6 due to degradation (e.g. hydrolysis) in the presence of clay. However, more detailed studies, including rheological studies in the very low shear rate region and polymer molecular weight characterization will be required to understand this behavior.

5. Thermal properties

The thermal properties of nylon 6 and the various composites were determined by differential scanning calorimetry, DSC, and thermogravimetric analysis, TGA. Table 3 provides a summary of the results. The DSC measurements indicate that the presence of filler does not affect the T_g of the nylon 6 matrix which occurs at approximately 53°C. The DSC melting peak (T_m) of the composites occurs at a slightly lower temperature than that of the neat nylon 6. This may be related to a slight reduction in crystallite size in the presence of fillers [28,47]. All of the fillers cause an increase in the crystallization temperature (T_c) relative to neat nylon 6. To various degrees, fillers may act as nucleating agents causing a higher crystallization rate than that of the neat nylon 6.

According to the TGA results in Table 3, the nanocomposites have somewhat lower stability than neat nylon 6. This is attributable to the degradation of the quaternary alkylammonium treatment on the montmorillonite. In the case of organoclay, the temperature at 5% weight loss is 271°C. However, Gilman et al. [48] observed that the fire retardant properties of nylon 6 nanocomposites were improved. In this case, the individual layers of clay act as an insulator and a mass transport barrier against oxygen or volatile degradation products generated as the nylon 6 decomposes. On the other hand, they did not find any differences in thermal stability.

6. Mechanical properties

6.1. Effect of filler type

Typical stress–strain diagrams for nylon 6 and

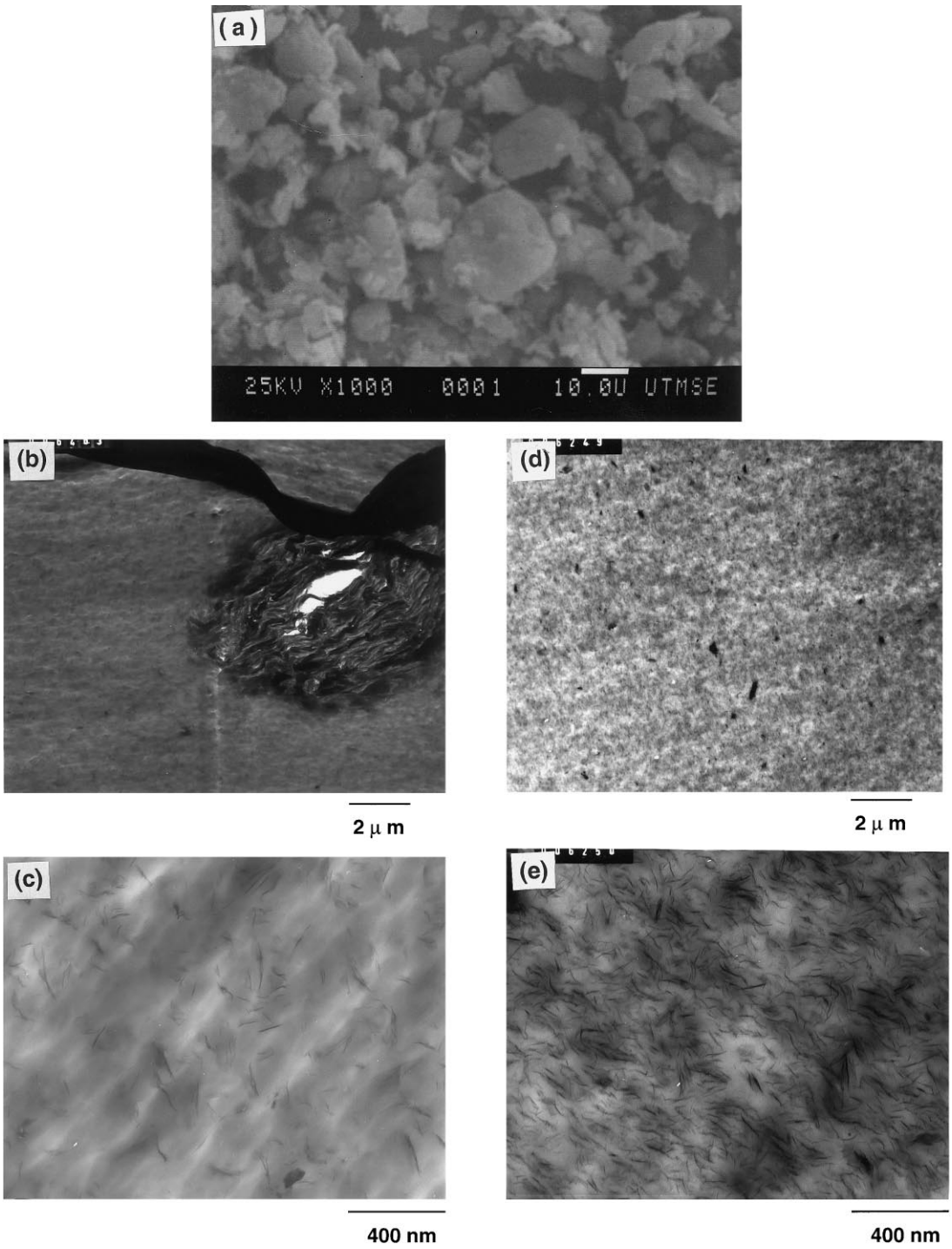

Fig. 3. SEM photomicrograph of (a) organoclay powder and TEM photomicrographs of nylon 6/organoclay 95/05 nanocomposites prepared by melt compounding using the single screw extruder at (b) low and (c) high magnification using the twin screw extruder at (d) low and (e) high magnification.

composites containing 5 wt% of fillers are shown in Fig. 5 (at 5.08 cm/min) and Fig. 6 (at 0.5 cm/min). A summary of the mechanical properties of these materials is shown in Table 4. The actual amount of mineral in each composite was measured by weighing the residue after burning them. As can be seen from Table 4, regardless of the type of filler, the strength and modulus were substantially increased relative to neat nylon 6 without significant variation in toughness or impact strength as measured by the standard Izod test. Furthermore, nanocomposites show superior mechanical properties, especially modulus as compared with conventional nylon 6 composites formed by compounding

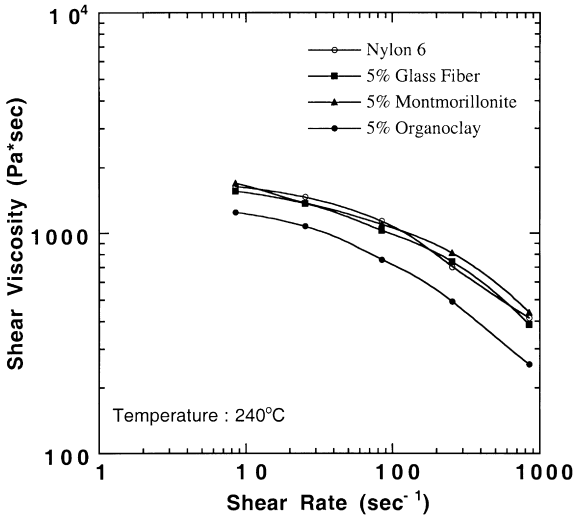

Fig. 4. Melt viscosity as a function of shear rate for the nylon 6 and composites at 240°C.

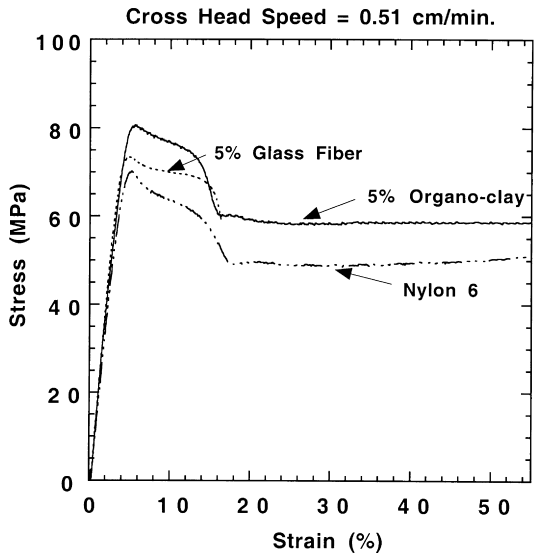

Fig. 6. Stress–strain curves for nylon 6 and 95/05 composites at a crosshead speed of 0.51 cm/min.

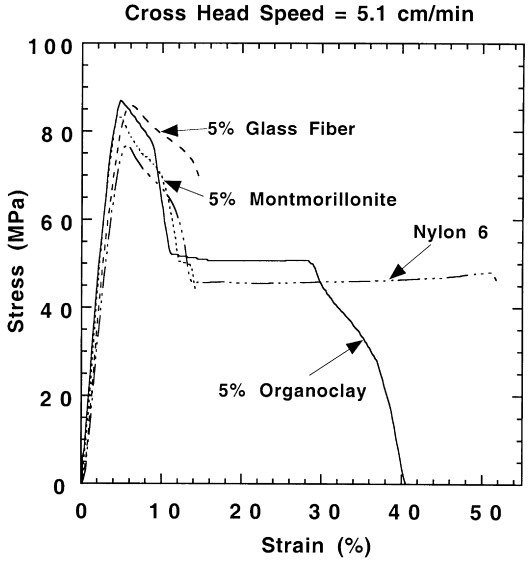

Fig. 5. Stress–strain curves for nylon 6 and 95/05 composites at a crosshead speed of 5.08 cm/min.

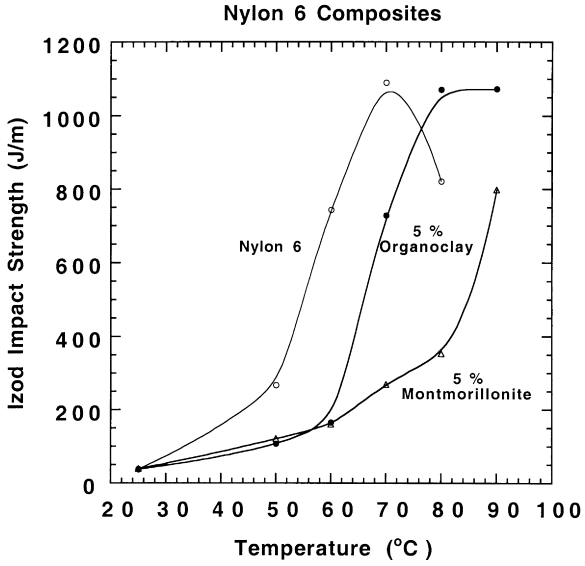

Fig. 7. Notched Izod impact strength of nylon 6 and 95/05 composites as a function of temperature.

Table 3
Thermal properties of nylon 6/filler composites

Polyamide composites	Filler (wt.%)	T_g[a] (°C)	T_m[b] (°C)	T_c[c] (°C)	T_d[d] (°C)
Nylon 6	0	53.1	221	165	420.3
N6/glass fiber	5	53.8	218	180	406.5
N6/montmorillonite	5	53.7	215	182	426.5
N6/organoclay	5[e]	50.8	217	178	411.7

[a] From second heat at a scan rate of 20°C/min using midpoint method.
[b] Melting temperature from DSC second heat at 20°C/min.
[c] Crystallization temperature measured on cooling at 20°C/min.
[d] Decomposition temperature determined by TGA (5% weight loss at scan late:20°C/min and N_2 atmosphere).
[e] Actual mineral content is 3.16% by weight.

Table 4
Mechanical properties of polyamide 6 composites

Polyamide composites	Mineral content (%)	Izod impact strength (J/m)	Modulus (GPa)	Yield strength (MPa)	Elongation at break (%)	
					Crosshead speed 0.51 cm/min	Crosshead speed 5.08 cm/min
Nylon 6	0	38 ± 4	2.66 ± 0.2	64.2 ± 0.8	200 ± 30	40 ± 8
N6/glass fiber	5	53 ± 8	3.26 ± 0.1	72.6 ± 0.8	18 ± 1.3	14 ± 4
N6/montmorillonite	5	40 ± 2	3.01 ± 0.1	75.4 ± 0.3	22 ± 6.0	14 ± 3
N6/organoclay	3.16	38 ± 3	3.66 ± 0.1	83.4 ± 0.7	126 ± 25	38 ± 19
N6/organoclay/glass fiber	8	44 ± 3	4.82 ± 0.1	95.0 ± 0.9	8 ± 0.5	7 ± 4

with glass fibers or untreated clay. The elongation to break for the nanocomposites is more or less the same as that of the neat nylon 6, whereas, those for the conventional composites are dramatically decreased. The elongation at break for the nanocomposites is greatly affected by crosshead speed as is the case for neat nylon 6; on the other hand, rate of extension has little effect on the elongation of glass fiber composites.

It is noteworthy that the composite of nylon 6 with untreated sodium montmorillonite clay shows far higher strength and modulus than neat nylon 6. This is quite contrary to the results from previous investigators who claim untreated clay composites with nylon 6 are inferior to neat nylon 6 in terms of some mechanical properties [13,49].

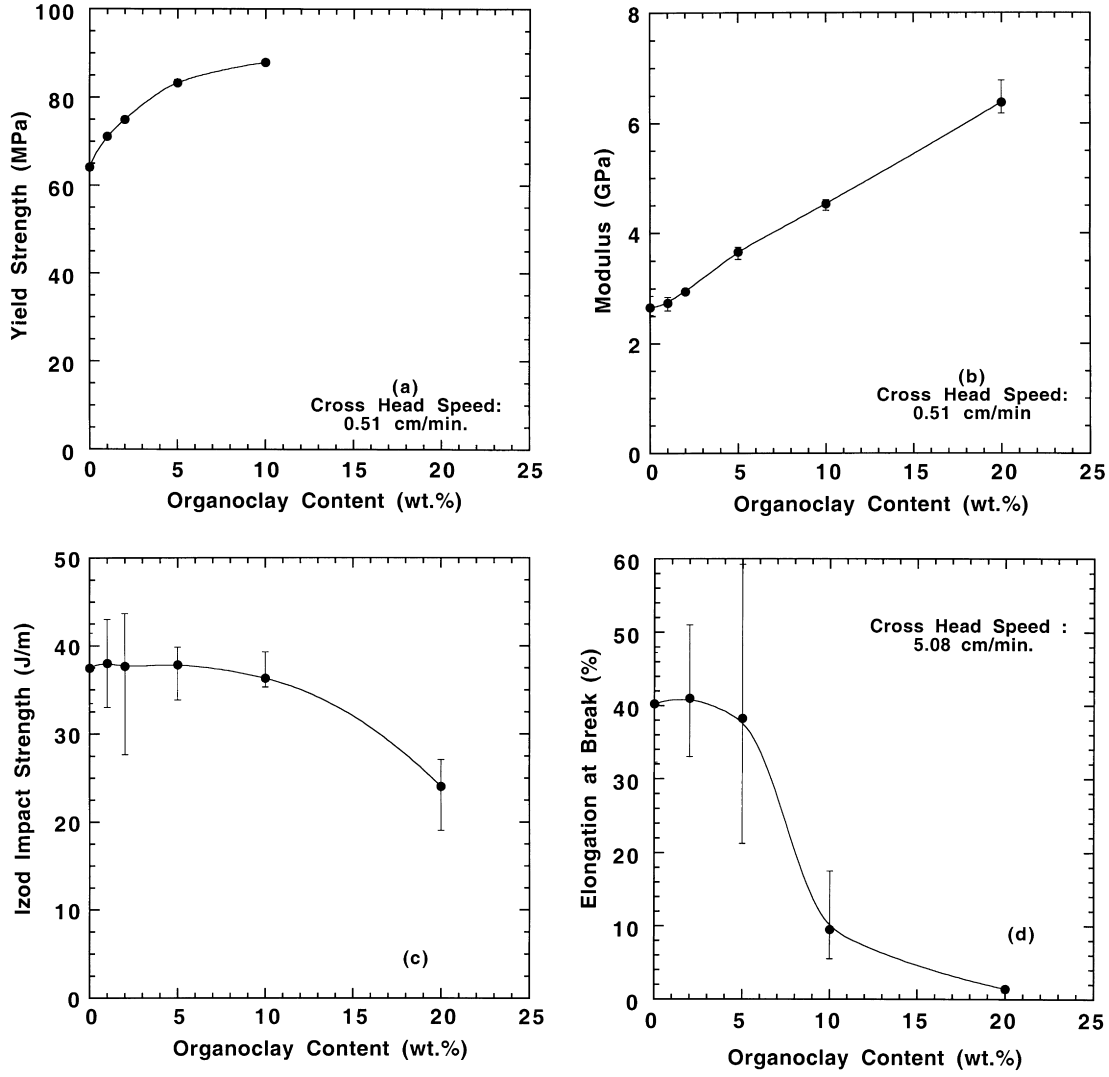

Fig. 8. Mechanical properties of melt processed nylon 6/organoclay nanocomposites as a function of organoclay content: (a) yield strength, (b) modulus, (c) Izod impact strength, (d) elongation to break.

Table 5
Mechanical properties of nylon 6/clay 95/05 composites with various processing parameters

Composition	Extruder type	Barrel temperature (°C)	Screw speed (rpm)	Izod impact strength (J/m)	Modulus (GPa)	Yield strength (MPa)	Elongation at break (%)
Nylon 6	Twin screw	240	180	38 ± 4	2.66 ± 0.2	64.2 ± 0.8	40 ± 8
N6/organoclay 95/05	Single screw	240	40	34 ± 5	3.47 ± 0.1	74.0 ± 1.6	12 ± 3
	Single screw (2 passes)	240	40	33 ± 8	3.53 ± 0.1	76.9 ± 0.4	13 ± 1
N6/organoclay	Twin screw	230	180	46 ± 6	3.66 ± 0.0	82.1 ± 0.8	29 ± 3
		240	80	41 ± 4	3.66 ± 0.2	82.4 ± 2.0	36 ± 9
		240	180	38 ± 3	3.66 ± 0.1	83.4 ± 0.7	38 ± 19
		240	280	47 ± 8	3.85 ± 0.1	87.6 ± 0.8	38 ± 19
		280	180	44 ± 6	3.72 ± 0.1	81.1 ± 0.6	32 ± 4
	Twin screw (2 passes)	240	180	56 ± 4	3.72 ± 0.1	85.7 ± 0.2	33 ± 6

Interestingly, there is a synergistic effect on the tensile strength and modulus when the exfoliated nanocomposite was used as the matrix for a glass fiber reinforced composite. As shown in Table 4, the modulus of the nanocomposite with 5 wt% loading of the organoclay is improved about 38% relative to neat nylon 6 and the glass fiber composite shows 22% improvement. When the glass fibers are added to the nanocomposite, the modulus is 81% higher than nylon 6; this exceeds what is expected based on simple additivity.

Fig. 7 shows the Izod impact strength as a function of temperature for nylon 6 composites containing 5 wt% of filler. The room temperature impact properties of each composite are similar to that of neat nylon 6; however, at higher temperatures, the Izod values for neat nylon 6 are higher than those of the composites based on organoclay which in turn are greater than those based on pure montmorillonite. All of these materials are super tough above the glass transition temperature of nylon 6.

6.2. Effect of organoclay content

Tensile and Izod impact properties were measured to evaluate the reinforcing effect of the organoclay. Fig. 8 summarizes these properties of the nylon 6 nanocomposites as a function of the organoclay content. Stiffness and strength are dramatically improved as the amount of organoclay increases. On the other hand, the impact strength and elongation at break values remain at the levels of neat nylon 6 up to about 5 wt% of the organoclay and then decrease thereafter. Mixtures containing 20 wt% organoclay are very brittle [40,50,51].

Fig. 9 shows the Izod impact strength as a function temperature for nylon 6 nanocomposites having different

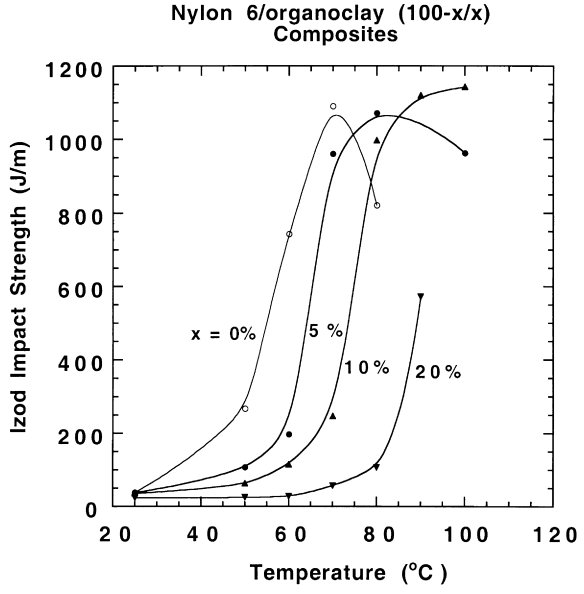

Fig. 9. Notched Izod impact strength for nylon 6/organoclay nanocomposites as a function of temperature.

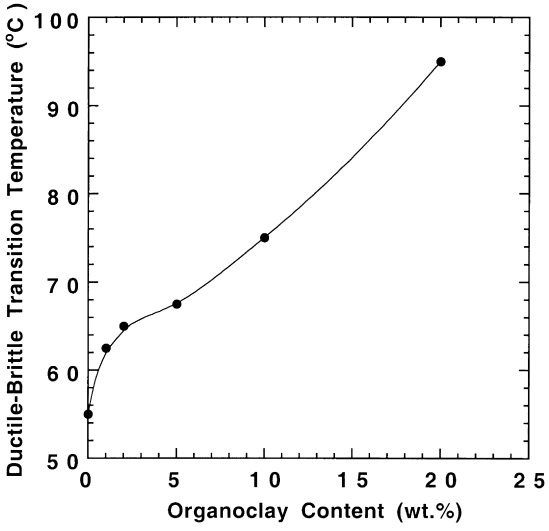

Fig. 10. Ductile–brittle transition temperature of nylon 6 nanocomposites as a function of organoclay content.

Table 6
Selected properties of various nylon 6/clay nanocomposites

Description	University of Texas		Alliedsignal		Chinese Academy of Science		Toyota			
Intercalating agent	SCPX 2004[a] Cloisite 30B[b]		Diphentyl Ammonium[a] 11-aminoundecanoic acid[b]		Octadecyl ammonium		12 Aminolauric acid			
Preparation	Twin screw melt compounding		Twin screw melt compounding		Twin screw melt compounding		In situ polymerization			
Composition	N6	N6/clay	N6	N6/clay	N6	N6/clay	N6	N6/clay	N6	N6/clay
Average M_n	29,300	29,300	29,300	29,300	N/A	N/A	N/A	N/A	20,000	15,000
Mineral content (wt.%)	0	3.16[a]; 3.40[b]	0	2.95[a]; 2.5[b]	0	5	0	10	0	4
Modulus (GPa)	2.66	3.66[a]; 4.30[b]	2.4	3.37[a]; 3.44[b]	3.0	4.1	1.74	3.26	1.11	1.87
Yield strength (MPa)	64.2	83.4[a]; 89.3[b]	66	80[a]; 80[b]	68.2	91.3	76	127	68.6	97.2
Elongation at break (%)	40	38[a]; 10[b]	26	44[a]; 12[b]	N/A	N/A	210	10	100	7.3

[a] Refers to data where SCPX 2004 was used.
[b] Refers to data where Cloisite 30B was used.

organoclay contents. As the temperature is increased to the region of the nylon 6 glass transition temperature, a brittle to ductile transition is observed even for the nanocomposites. When the matrix is above its T_g, the nanocomposites are super tough indicating high levels of ductility. The ductile–brittle transition temperatures deduced from the data in Fig. 9 (the mid-point of the step change in impact strength) are shown in Fig. 10 as a function of organoclay content. The ductile–brittle transition temperature is substantially increased by addition of organoclay.

6.3. Effect of processing

The effect of the mixer type and processing parameters on the various mechanical properties of nanocomposites are shown in Table 5. In the case of composites formed in the single screw extruder, see Fig. 3b, the exfoliation of the clay platelets is not extensive. Even after a second pass through this extruder, undispersed tactoids are still easily observed with the naked eye. On the other hand, the tensile strength and modulus of the organoclay composite produced by the second pass are improved slightly whereas the elongation at break and Izod impact strength of this composite are not improved by the second extrusion pass. As indicated in Table 5, nylon 6 nanocomposites with good properties can be obtained over a broad range of processing conditions in the twin screw extruder. The final nanocomposite properties are almost independent of the barrel temperature over the range of typical nylon 6 processing (230–280°C). The mechanical properties are slightly improved by increasing the screw speed, or a second pass through the extruder. Therefore, processing conditions need to be optimized to allow greater exfoliation of the clay platelets. It appears that there needs to be a long enough residence time and an appropriate shear history for best delamination of the clay. According to Lan and Pinnavaia [52,53], the exfoliated clay nanocomposites exhibit better mechanical performance than intercalated analogues.

6.4. Benchmarking with previous studies

The data in Table 6 show selected mechanical properties of nylon 6 nanocomposites reported in the literature [8,19,38,40,42] along with those determined here. Much of the prior literature has focused on nylon 6/clay nanocomposites formed by in situ polymerization. The purpose here is to compare the properties of the materials prepared here with those made by in situ polymerization and from other limited reports of melt processed materials. Table 6 shows the properties of typical materials from the literature. Regardless of preparation method or type of organoclay, the modulus and strength of the nanocomposites are significantly enhanced relative to those reported for neat nylon 6. It is difficult to make direct comparison of absolute property values among the materials reported from different

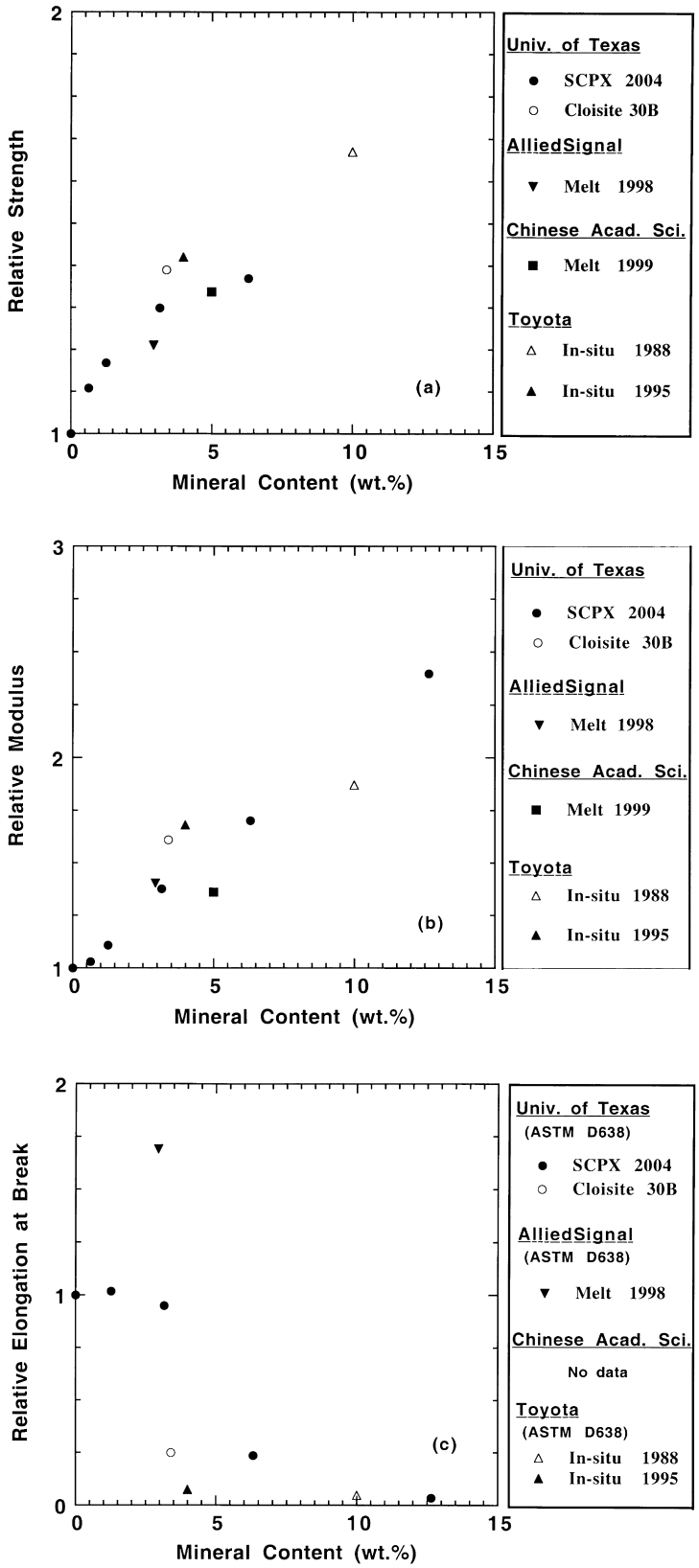

Fig. 11. Relative mechanical properties of various nylon 6 nanocomposites as a function of mineral content: (a) yield strength, (b) modulus, (c) elongation at break.

laboratories because of several factors. First, the mineral contents of the various organoclays are different and the nanocomposites do not contain exactly the same amounts of clay mineral. Secondly, there are evidently differences in methodologies by each laboratory since the reported properties of the neat nylon 6 vary widely. Thus, we use the strategy of plotting the relative property (nanocomposite value divided by that of neat nylon 6 reported in each paper or patent) versus the mineral content, see Fig. 11. This approach allows comparison of properties at equivalent mineral content using limited data. As shown in Fig. 11a and b, the relative stiffness and strength of the materials prepared here by melt processing are quite comparable with those from the literature. The relative elongation at break values show a lot of variability as might be expected since this is a flaw and rate sensitive property, see Fig. 11c. The relative elongation at break values for the materials prepared here remain at the levels of neat nylon 6 up to about 3 wt.% mineral content then decrease thereafter. Surprisingly, the elongation at break of the nanocomposite prepared by melt processing using an organoclay containing a secondary ammonium cation reported by AlliedSignal seems to have greater ductility than neat nylon 6; this observation needs to be explored further. Limited data from our laboratory suggest a strong dependence of the organoclay type (compare SCPX 2004 versus Cloisite 30B) on ductility. Interestingly, the materials from Toyoto prepared by in situ polymerization have low ductility.

7. Conclusions

Nylon 6–organoclay nanocomposites were prepared by melt compounding using a typical co-rotating twin screw extruder and compared with composites containing glass fibers and untreated clay. Transmission electron microscopy and X-ray diffraction indicate that the organoclay was well dispersed into the nylon 6 matrix and the mechanical properties of these materials compare well with those from the literature for nanocomposites formed by in situ polymerization and by melt processing. Melt processing in a single screw extruder failed to give similar levels of dispersion or exfoliation.

A high degree of exfoliation by melt processing seems to require an adequate residence time in the extruder and appropriate shear history. While well exfoliated nanocomposites show continuous improvement in strength and modulus relative to the neat nylon 6 matrix as more organoclay is added, there appears to be a loss of ductility beyond a certain mineral loading. The type of organotreatment and the speed of testing seem to have significant effects on ductility; both issues will be addressed in greater detail in future studies. Addition of organoclay to nylon 6 significantly increases the ductile-to-brittle transition temperature. Brief comparisons to glass fiber composites were made.

Acknowledgements

This material is based in part upon work supported by the Texas Advanced Technology program under Grant number 003658-0017 and 0067. The authors would like to thank Southern Clay Products Inc., for providing clay materials, XRD, TEM analyses, and for many helpful discussions. We also would like to thank the University of Akron for use of the Instron Capillary Rheometer.

References

[1] Pinnavaia TJ. Science 1983;220:365.
[2] Mehrotra V, Giannelis EP. Mater Res Soc Symp Proc 1990;171:39.
[3] Giannelis EP. J Minerals, Metals Mater Soc 1992;44:28.
[4] Carter LW, Hendricks JG, Bolley DS. United States Patent No. 2531396 (1950) (assigned to National Lead Co.).
[5] Nahin PG, Backlund PS. United States Patent No. 3084117 (1963) (assigned to Union Oil Co.).
[6] Fujiwara S, Sakamoto T. Japanese Kokai Patent Application No. 109998 (1976) (assigned to Unichika K.K., Japan).
[7] Fukushima Y, Inagaki S. J Inclusion Phenomena 1987;5:473.
[8] Okada A, Fukushima Y, Kawasumi M, Inagaki S, Usuki A, Sugiyama S, Kurauch T, Kamigaito O. United States Patent No. 4739007 (1988) (assigned to Toyota Motor Co., Japan).
[9] Kawasumi M, Kohzaki M, Kojima Y, Okada A, Kamigaito O. United States Patent No. 4810734 (1989) (assigned to Toyota Motor Co. Japan).
[10] Usuki A, Kojima Y, Kawasumi M, Okada A, Fukushima Y, Kurauch T, Kamigaito O. J Mater Res 1993;8:1179.
[11] Usuki A, Mizutani T, Fukushima Y, Fujimoto M, Fukumori K, Kojima Y, Sato N, Kurauch T, Kamigaito O. United States Patent No. 4889885 (1989) (assigned to Toyota Motor Co., Japan).
[12] Okada A, Fukumori K, Usuki A, Kojima Y, Sato N, Kurauchi T, Kamigaito O. ACS Polym Preprints 1991;32:540.
[13] Okada A, Usuki A. Mater Sci Engng C 1995;3:109.
[14] Yano K, Usuki A, Okada A, Kurauch T. United States Patent No. 5164460 (1992) (assigned to Toyota Motor Co., Japan).
[15] Yano K, Usuki A, Okada A. J Polym Sci Part A; Polym Chem 1997;35:2289.
[16] Kojima Y, Usuki A, Kawasumi M, Okada A, Fukushima Y, Kurauch T, Kamigaito O. J Mater Res 1993;8:1185.
[17] Kojima Y, Fukumori K, Usuki A, Okada A, Kurauchi T. J Mater Sci Lett 1993;12:889.
[18] Kojima Y, Usuki A, Kawasumi M, Okada A, Kurauch T, Kamigaito O. J Appl Polym Sci 1993;49:1259.
[19] Usuki A, Koiwai A, Kojima Y, Kawasumi M, Okada A, Kurauch T, Kamigaito O. J Appl Polym Sci 1995;55:119.
[20] Vaia RA, Ishii H, Giannelis EP. Chem Mater 1993;5:1694.
[21] Vaia RA, Jandt KD, Kramer EJ, Giannelis EP. Macromolecules 1995;28:8080.
[22] Akelah A, Moet A. J Mater Sci 1996;31:3589.
[23] Wang MS, Pinnavaia TJ. Chem Mater 1994;6:468.
[24] Lan T, Pinnavaia TJ. Chem Mater 1994;6:2216.
[25] Messersmith P, Giannelis EP. Chem Mater 1994;6:1719.
[26] Biasci L, Aglietto M, Ruggeri G, Ciardelli F. Polymer 1994;35:3296.
[27] Messersmith PB, Giannelis EP. J Polym Sci Part A: Polym Chem 1995;33:1047.
[28] Jimenez G, Ogata N, Kawai H, Ogihara T. J Appl Polym Sci 1997;64(11):2211.
[29] Kurokawa Y, Yasuda H, Oya A. J Mater Sci Lett 1996;15:1481.

[30] Furuichi N, Kurokawa Y, Fujita K, Oya A, Yasuda H, Kiso M. J Mater Sci 1996;31:4307.
[31] Kurokawa Y, Yasuda H, Kashiwagi M, Oya A. J Mater Sci Lett 1997:1670.
[32] Jeon H, Jung H, Lee S, Hudson S. Polym Bull 1998;41:107.
[33] Wang Z, Pinnavaia TJ. Chem Mater 1998;10:3769.
[34] Zhu Z, Yang Y, Yin J, Wang X, Ke Y, Qi Z. J Appl Polym Sci 1999;73:2063.
[35] Vaia RA, Giannelis EP. Macromolecules 1997;30:7990.
[36] Vaia RA, Giannelis EP. Macromolecules 1997;30:8000.
[37] Maxfield M, Christiani BR, Murthy SN, Tuller H. United States Patent No. 5385776 (1995) (assigned to AlliedSignal Inc.).
[38] Christiani BR, Maxfield M. United States Patent No. 5747560 (1998) (assigned to AlliedSignal Inc.).
[39] Kawasumi M, Hasegawa N, Kato M, Usuki A, Okada A. Macromolecules 1997;30:6333.
[40] Liu L, Qi Z, Zhu X. J Appl Polym Sci 1999;71:1133.
[41] Bolen WR, Colwell RE. SPE J 1958;14:24.
[42] Dennis H.R., Hunter D.L., Chang D., Kim S., White J.L., Cho J.W., Paul D.R.. SPE Antec Tech Papers 2000;40:428.
[43] Krishnamoorti R, Vaia A, Giannelis EP. Chem Mater 1996;8:1728.
[44] Krishnamoorti R, Giannelis EP. Macromolecules 1997;30:4097.
[45] Krishnamoorti R. ACS Polym Preprints 1999;40:122.
[46] Solomon MJ, Seefeldt KF, Almusallam A, Varadan P. Effect of microstructure on the rheology of polypropylene/clay nanocomposites, AIChE Annual Meeting, Dallas, TX, November 1999.
[47] Ogata N, Kawakage S, Ogihara T. Polymer 1997;38(20):5115.
[48] Gilman JW, Kashiwagi T, Lichtenhan JD. Int SAMPE Symp 1997;42:1078.
[49] Yang F, Ou Y, Yu Z. J Appl Polym Sci 1998;69:355.
[50] Ou Y, Yang F, Yu Z. J Polym Sci Part B: Polym Phys 1998;36:789.
[51] Yang F, Ou Y, Yu Z. J Appl Polym Sci 1998;69:355.
[52] Lan T, Kaviratna PD, Pinnavaia TJ. Chem Mater 1995;7:2144.
[53] Lan T, Pinnavaia TJ. Mater Res Soc Symp Proc 1996;435:79.